Adapting Shot Peening for Surface Texturing Using Customized Additive Manufactured Shots

Asghar Heydari Astaraee, Sara Bagherifard, Emilio Alfredo Rajme López, and Mario Guagliano*

Surface textures in engineering materials not only affect the reflective properties and aesthetics but if properly designed can modulate surface-related properties such as wettability, fatigue, wear, corrosion, and scratch resistance. Herein, a new surface texturing method is introduced based on the conventional shot peening process. Custom shots are designed, and their surface texturing capability is investigated on acrylonitrile butadiene styrene (ABS) polymer substrates. A finite-element model is developed to bombard the substrate using AISI 316 stainless steel customized shots. The generated unique textures are compared qualitatively by visual examination and quantitatively using the standard surface roughness parameters. As a proof of concept, preliminary experiments are performed using a candidate custom shot and a spherical shot to treat the ABS sheets. The results highlight the high potential of the shot peening technique paired with additive manufacturing for customizing the peening media to be used for surface texturing polymeric materials.

1. Introduction

Shot peening (SP) is a well-recognized efficient surface treatment, which induces plastic deformation in the surface layer of a metallic substrate by repeated impacts of metallic, ceramic, or glass peening media. As a result of successive plastic deformations, compressive residual stresses are generated near the shot peened surface, and consequently, the surface roughness and morphology are altered.[1] Also, a work-hardened layer with possible grain refinement is introduced upon the application of SP.[2] Generally, SP is intended to increase the lifetime of metallic components under cyclic loading.[3,4] The proper selection of process parameters is essential for achieving desired results while the Almen intensity, being an indicator of the kinetic

energy of the media flow, is the most important control parameter, together with surface coverage that is related to exposure time.[5]

When it comes to polymeric materials, the usage of SP has not been widespread. There are a few investigations on the application of SP to polymeric substrates. A study on the effect of SP applied to epoxy resin composite reinforced by electrical glass fibers revealed that the tensile and fatigue strength of the substrates was improved by around 30–60% at certain SP coverages.[6] SP was applied as an interlayer process for additive manufacturing (AM) of acrylonitrile butadiene styrene (ABS) using fused filament fabrication (FFF).[7] The results showed that the hybrid fabrication approach was effective in enhancing the dynamic properties tested by Charpy impact and drop weight tests. However, it caused a reduction in stiffness. In another study,[8] it was reported that coupling SP with FFF reduced the tensile strength but increased the elongation. It was concluded that overpeening or peening by recycled media easily damaged the surface of the polymeric materials. In addition, the favorable compressive residual stress fields were not necessarily produced as is the case for metals.

Even though it may not be straightforward to take benefit from the residual stresses or work hardening induced by SP in polymers due to the different nature of the material, SP can be still utilized for altering their surface morphology. As a direct outcome of SP, the permanent deformation induced on the surface generates a distinct surface morphology. To a broader extent, the concept of surface texturing has emerged to accomplish novel demands in various areas including surface engineering.[9] Surface texturing modifies the surface with the primary aim to generate patterns or textures with tiny features on the material surface to improve superficial functionalities.[10] These can include scratch and mar resistance,[11] tribological properties,[12] biological characteristics,[13] and energy-related performances such as wettability and capillarity,[14] let alone aesthetics. The type and size of the generated features depend on the specific texturing technique. Several techniques such as ion-beam etching,[15] electrochemical machining, micromilling, lithography, laser processing,[16] hot embossing,[17] and mechanical texturing have been studied in the past, especially on polymeric materials. The great variety of surface modification methodologies commonly available today highlights the importance to achieve specific

A. Heydari Astaraee, S. Bagherifard, E. A. Rajme López, M. Guagliano
Department of Mechanical Engineering
Politecnico di Milano
20156 Milan, Italy
E-mail: sara.bagherifard@gmail.com

The ORCID identification number(s) for the author(s) of this article can be found under https://doi.org/10.1002/adem.202201730.

**ADVANCED
SCIENCE NEWS**

www.advancedsciencenews.com

**ADVANCED
ENGINEERING
MATERIALS**

www.aem-journal.com

surface properties to control roughness and texture, that can affect the surface's reflective properties, hardness, lubricant retention, drag force control, and structural integrity, just to name a few examples.

The idea behind this study is to assess the potential of SP to be considered a candidate for the mechanical surface texturing of polymers by inducing surface plastic deformation using customized shots. In contrast to many other techniques, SP does not involve material removal, does not need high temperatures or pressures, and can be relatively fast, cheap, and sustainable with a high capacity for industrialization. The need to customize shots could enhance the overall cost, but there are alternative peening apparatuses that can mediate this aspect, as discussed in this work. In this study, the capabilities of SP are explored by evaluating the possibility of surface texturing of ABS using custom AM shots. Various shot designs are proposed, and the created surface textures are studied both numerically and experimentally in terms of morphology and standard surface roughness.

2. Experimental Section

2.1. Shot Proposals

Traditionally in SP, spherical, semispherical, or cut-wire (cylindrical) shots were used as the peening media with typical dimensions lower than 1 mm. More recently, larger shots (1–10 mm in diameter) were used in peening-based surface nanostructuring techniques such as ultrasonic SP (USP), known also as surface mechanical attrition treatment (SMAT).[18] Since what deforms the surface in SP is the media impacting with high kinetic energy, thus, to explore the ability of SP to generate customized surface textures, 3D shots with elaborate patterns should be designed. The custom shot designs developed in this study are illustrated in **Figure 1**. The idea behind the shot designs was to produce hierarchical surface deformation, that is, creating smaller indents inside a larger spherical indentation. Thus, innovative features such as bumps or indents were added to the basic spherical shot. The design proposals passed a trial-and-error design finite-element (FE) modeling stage to make sure that the polymeric surface was peened homogenously without any severe deformations. The basic shape of the shots was spherical, and the geometrical features were added to the surface to render them unique. The nominations of the proposed shots were inspired by their expected output layout, which was a sphere, football, multibumps, golf ball, icosahedron, lattice, and square-patterned shot. Laser powder bed fusion (LPBF) is considered as the candidate method for the manufacturing of customized shots. Thus, the manufacturing limitations of the LPBF

process were taken into account when designing the shot geometries. All the designs had an overall diameter of around 8 mm. The football design, which was a truncated icosahedron, had an inner diameter of 7 mm and a fillet radius of 0.1 mm. The multibumps shot consisted of bumps with a diameter and maximum height of 1.3 and 0.25 mm, respectively. The golf ball was a counterpart of the multibumps shot, which consisted of a solid spherical core with dimples over its surface. This shot intended to create small bumps on the peened polymeric surface. The spherical core had a diameter of 8 mm, and the dimples were set 3.8 mm away from the sphere center with a diameter of 1.7 mm and a fillet radius of 0.25 mm. The lattice shot had a geometrical transition along its different zones, starting from triangles, continuing with curved rhombuses, and finally, ending in squares. Its geometry consisted of a solid spherical core of 7.6 mm and an array of crossed rings over its surface with a radius of 0.5 mm. All the fillets had a radius of 0.1 mm. Finally, also in the square-patterned shot, the transition between geometric figures was exploited. However, instead of using a lattice of rings, the hard lines define the transition from triangles at the top to squares in the middle. This design consisted of a gem-like core with bas-relief cuts and chamfer angles of 75°.

2.2. Numerical Modeling

Numerical simulations were performed using Abaqus Explicit 2019 FE software with a dynamic explicit procedure that allows analyzing realistic deformations of brief transient dynamic events. The geometrical features of the model are shown in **Figure 2**a. The shot geometries were created using SolidWorks 2020 and imported into Abaqus. Then, they were converted into solid shells to save computational time. This assumption is valid due to a large difference between the stiffness of the steel shots and the polymeric substrate, which allows the modeling of the shot as a rigid body. The substrate was modeled using a slab with dimensions of $40 \times 40 \times 5$ mm^3. The thickness was assigned according to the thickness of the real material sheet, used in the experiments (Section 2.3.1). The impact area was selected to be 10×10 mm^2 in the center of the substrate model. Semi-infinite elements were introduced in the four side faces of the substrate to model a large body and reduce the effect of stress waves reflected from the boundaries while all the translational and rotational boundary conditions of the bottom face were fixed. The target was meshed using 3D stress elements of C3D8R and infinite elements of CIN3D8 while the shots were meshed using S4R elements. After a mesh convergence study, the element size on the shot as well as in the impact area was selected to be 0.04 mm.
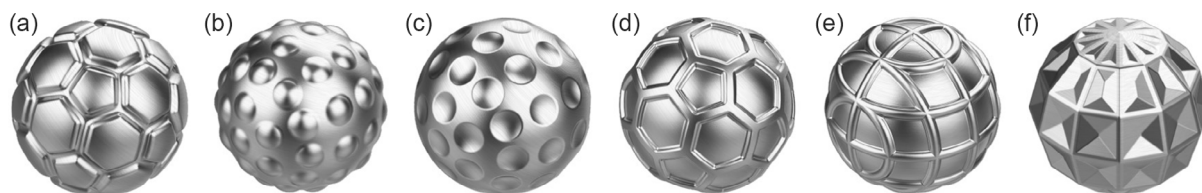
Figure 1. The proposed designs of the custom AM-fabricated shots: a) football, b) multibumps, c) golf ball, d) icosahedron, e) lattice, and f) square patterned.
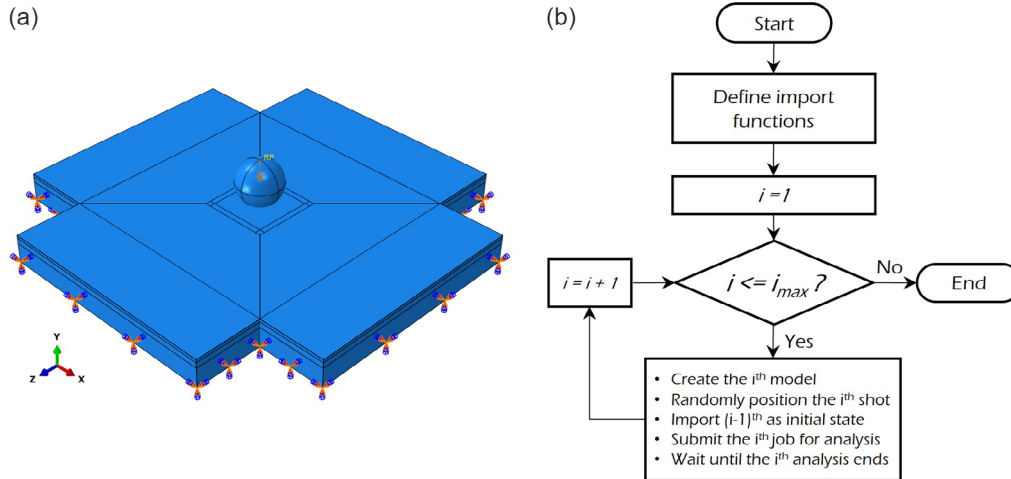
Figure 2. a) Geometry of the FE model with a spherical shot and boundary conditions. b) The algorithm of the multishot impact model.

Table 1. Material properties of ABS and stainless steel.

Material	Density [g cm^{-3}]	Young's modulus [GPa]	Poisson's ratio	A [MPa]	B [MPa]	n	m	C	$\dot{\varepsilon}_0$ [s^{-1}]
ABS[20]	1.04	2.5	0.35	39	48	1.5	0.879	0.053	8×10^{-4}
Steel	7.8	–	–	–	–	–	–	–	–

The mass of the shots was defined using a density equal to 7.8 g cm^{-3}. The viscoplastic behavior of the ABS polymer was implemented using the Johnson–Cook plasticity model[19] from which the constants were derived,[20] as listed in **Table 1**.

Shot impact velocities typically in air blast peening and rotary wheel peening are commonly selected in the order of 20–150 m s^{-1} depending on the media and substrate material and the desired Almen intensity.[21] However, the large shots (8 mm in diameter) considered in the current study cannot be used in the classic SP and the imposed velocity should be here adapted to the shot dimension. The selected shot size is more adapted for the case of USP and SMAT, which use shots in the range of 1–10 mm in diameter to peen the material and induce grain refinement in the surface layer. The average shot velocity in these processes was estimated to be in the range of 1–10 m s^{-1} depending on the processing parameters.[22,23] Based on the earlier discussion, a constant shot velocity equal to 10 m s^{-1} was selected and assigned to the shots as an initial boundary condition in the simulations. In addition, to explore the effect of lower velocity on the roughness and surface texture, simulations were performed for two of the custom shots (lattice and square patterned) using also an impact velocity of 5 m s^{-1}. The angle of impact was set as 90° concerning the impact area in all cases, as it is typical for SP.

To obtain an idea regarding the required number of impacts and its relation with peening coverage, the Kirk–Abyaneh model was utilized.[24] This model used the dimple size produced by a single shot impact over the target surface to estimate the required number of impacts to reach the desired peening coverage. The details of the calculations can be found in a previous study.[25]

The multishot impact model was created using a Python script, the outline of which is indicated in Figure 2b. In this script, a single-shot impact model was created with a randomly positioned shot, and the results of the previous impact were imported into this model. Each single-shot model was run until the impact was completed and the shot detached from the substrate after the rebound. This loop was continued until the required number of impacts to achieve a preset surface coverage was simulated. For a realistic simulation of the peening process, in addition to considering random impact positions for the shots by defining the coordinates on the surface of impact, random angular rotation around their axes was also considered.
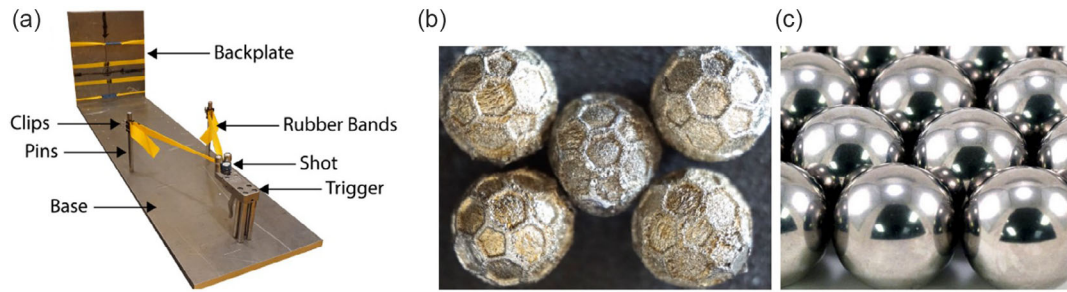
2.3. Experimental Analysis

2.3.1. Peening Experiments

A set of preliminary experimental tests were performed based on a simple slingshot system to provide proof of concept. **Figure 3**a shows the setup and the related components. The slingshot used an aluminum plate as a base to fix the pins and the trigger. The rubber band was placed around the pins and kept in place with clips.

A backplate was installed at the end of the base where the polymeric target (5 mm in thickness) was positioned and fixed. Two different shot geometries were considered: custom shots of icosahedron manufactured by LPBF technology using 316 stainless steel powder and spherical AISI 316 stainless steel ball bearings of 8 mm in diameter, for reference (Figure 3b,c).

The principle of energy conservation was used to estimate the impact velocity of the shot. Some assumptions such as no friction, no change in the vertical position, and no heat loss were considered to facilitate the calculations. The total energy of the system (E_M) is the sum of the potential energy stored in the rubber band (E_P) and the kinetic energy of the motion (E_K). The phenomenon can be split into two states: the first is the motionless shot (zero kinetic energy) pulled backward to a determined distance giving tension to the rubber band and

ADVANCED
SCIENCE NEWS
www.advancedsciencenews.com

ADVANCED
ENGINEERING
MATERIALS
www.aem-journal.com

Figure 3. a) Slingshot system used for the preliminary peening experiments. b) Icosahedron custom shots (around 8 mm in diameter) manufactured by LPBF technology in their AB condition. c) Spherical stainless steel ball bearings (8 mm in diameter).

the second is the flying shot completely detached from the rubber bands (zero potential energy). The conservation of mechanical energy says that the energy in state one should be equivalent to the mechanical energy in the second state, defined by the following equations.

$$E_{M1} = E_{M2} \tag{1}$$

$$E_{P1} + E_{K1} = E_{P2} + E_{K2} \tag{2}$$

Because of the zero kinetic energy in state one and the zero potential energy in state two, $E_{K1} = 0$ and $E_{P2} = 0$, which gives the following form

$$E_{P1} = E_{K2} \tag{3}$$

The potential energy stored by the rubber band and the kinetic energy of the flying shot can be expressed respectively as follows

$$E_{P1} = \frac{1}{2} \cdot k \cdot x^2 \tag{4}$$

$$E_{K1} = \frac{1}{2} \cdot m \cdot v^2 \tag{5}$$

where k is the rubber band's stiffness constant, x is the elongation of the rubber band, m is the mass of the shot, and v is the speed to be estimated by rearranging the equations as follows.

$$v = \sqrt{\frac{k \cdot x^2}{m}} \tag{6}$$

The elastic constant of the rubber band was experimentally determined with tensile tests aimed at finding the force–elongation (F–x) relation

$$F = k \cdot x \tag{7}$$

where F is the force exerted by the rubber band, k is the spring stiffness constant, and x is the elongation. Finally, substituting Equation (7) in Equation (6) gives the final form

$$v = \sqrt{\frac{F \cdot x}{m}} \tag{8}$$

A dynamometer and a measuring tape were used to experimentally determine the force and the elongation. **Table 2** shows the parameters that provided the desired impact velocities to be

Table 2. Parameters to estimate the steel shot velocity in the slingshot system.

Elongation x [mm]	Force F [N]	Stiffness K [N m^{-1}]	Potential energy $P.E.$ [J]	Mass m [kg]	Estimated velocity v [m s^{-1}]
25	2.5	100	0.045	0.002	5.6 $\pm$ 0.3
45	4.5	100	0.125	0.002	10.1 $\pm$ 0.5
65	6.5	100	0.245	0.002	14.5 $\pm$ 0.7

similar to the one imposed in the numerical models, calculated by Equation (8). The tests were repeated for three times and the indicated deviation in velocity was calculated based on the error propagation.
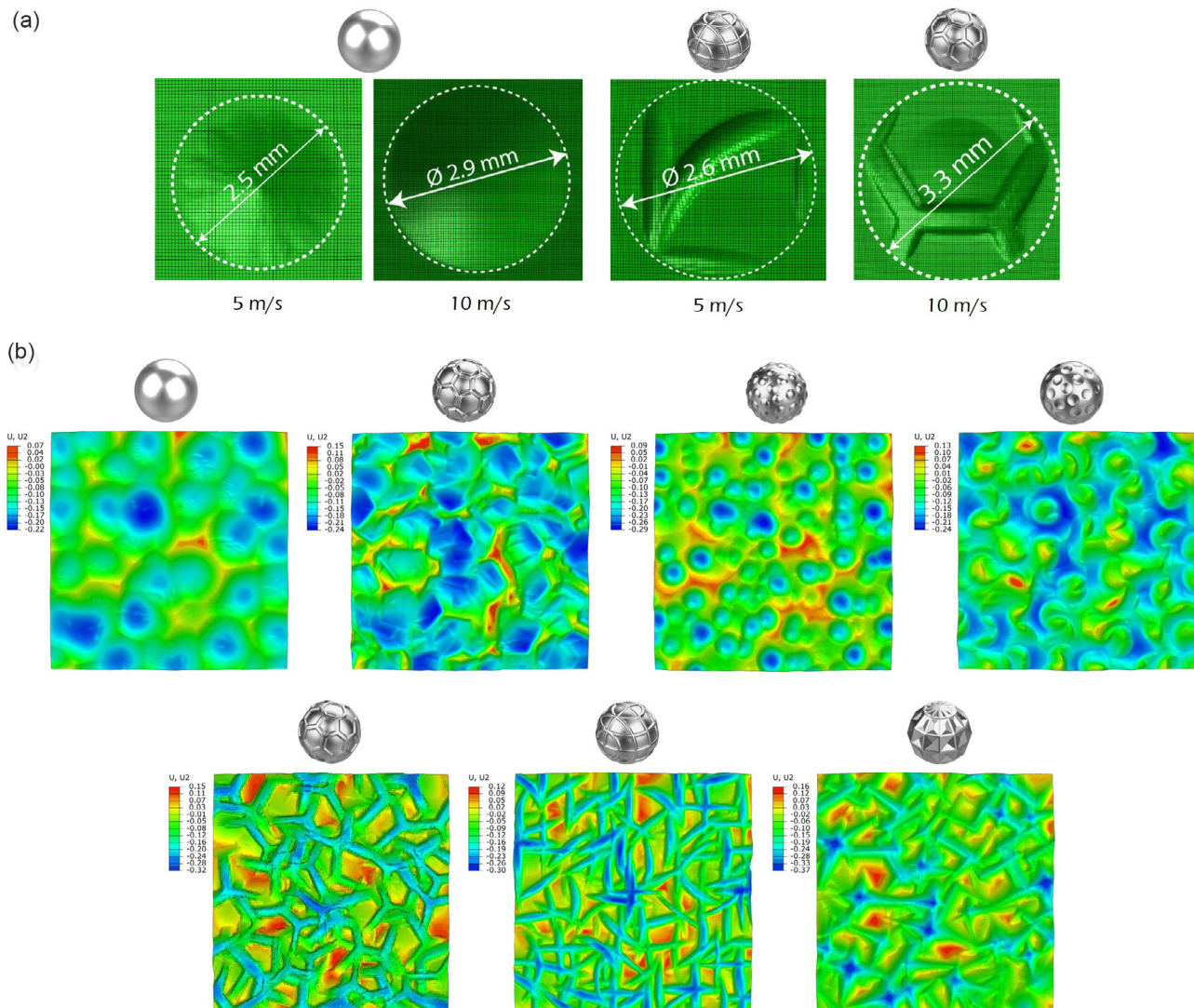
2.3.2. Surface Roughness Measurement

To quantify the surface roughness of the treated surfaces with the slingshot system, a Bruker Alicona InfiniteFocus 3D noncontact optical device was used. The measurements were performed on the surfaces treated with an impact velocity of 10.1 m s^{-1} within an area of 5 × 5mm^2 both using the spherical shot and the icosahedron shot. This area size was used to make sure that the measurements were performed within the peened area. The measurements were repeated three times using different areas over the peened surface to evaluate the repeatability. The cutoff length used in the measurements was 1.03 mm, which was calculated automatically by the device. Areal amplitude parameters including arithmetic mean height (Sa), root mean square height (Sq), maximum peak height (Sp), maximum valley height (Sv), maximum peak to valley height (Sz), and ten-point height average (S10z) were measured according to the ISO 25 178-2.[26]

3. Results

The sizes of the dimples produced by the spherical shot obtained by FE simulation were estimated to be 2.5 and 2.9 mm for shot velocities of 5 and 10 m s^{-1}, respectively (**Figure 4**a). Thus, according to the coverage model of Kirk–Abyaneh,[24] the required number of shots to produce a fully covered surface (to be considered as 98% coverage based on agreed conventions) was assessed to be 60 and 74, for the velocities of 5 and 10 m s^{-1}, respectively. Two typical dimples generated by the lattice and

ADVANCED
SCIENCE NEWS
www.advancedsciencenews.com

ADVANCED
ENGINEERING
MATERIALS
www.aem-journal.com

Figure 4. a) Dimples created by a single-shot impact for the spherical, lattice, and icosahedron shots at different impact velocities (deformation scale factor = 1). b) Resultant displacement contours (in millimeters) in the y direction at a shot velocity of 10 m s^{-1} and 60 impacts for different shot designs. All shots have a diameter of around 8 mm.

icosahedron shot designs, respectively, at 5 and 10 m s^{-1}, are also depicted in Figure 4a. It is observed that for the custom shots, the surface dimples are irregular in shape due to the specific geometrical features of each shot. In addition, it can be envisaged that the dimples are not unique since they are dependent on the rotational angle of the shot. This, in turn, imposes a complex procedure for coverage estimation. For this reason and within the scope of this study, the same impact numbers calculated for the spherical shot were utilized for the custom shots regarding the relevant impact velocity. This implies that a fixed peening duration was assumed for all the shots to achieve the desired surface coverage at a certain impact velocity. The vertical displacement contours obtained after 60 consecutive impacts are shown in Figure 4b for all the shot designs, including for the football, multibump, golf ball, icosahedron, lattice, and square-patterned shots. It is observed that each custom shot has the potential of

inducing a distinct texture with entirely unique aesthetic features on the target surface.

Figure 5 shows the evolution of the surface texture induced by SP at an impact velocity of 10 m s^{-1} using different custom shots as a function of the number of impacts. As the reference case, the resultant textures from the solid sphere shot are also presented (Figure 5a). Figure 5b–g shows the texture evolution for the football, multibump, golf ball, icosahedron, lattice, and square-patterned shots, respectively. In general, it is found that by increasing the impact number from 30 to 60, the induced features over the surface become denser, and more uniform, despite being random in nature.

To quantify the surface morphology of the developed textures obtained from the numerical simulations, standard areal roughness parameters were exploited. The surface roughness of the simulated textures was postprocessed using a code developed
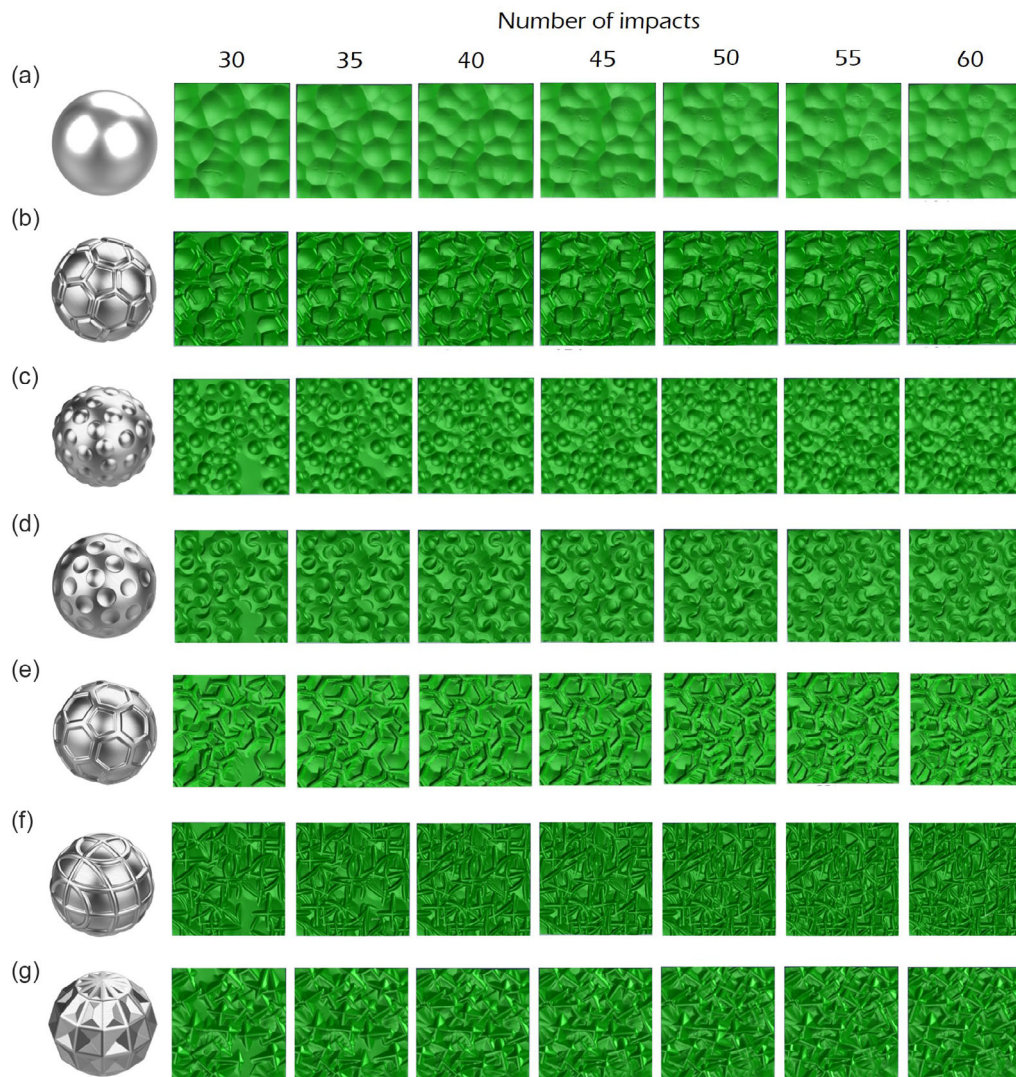
Figure 5. Evolution of the numerical surface texture induced by SP as a function of impact number with an impact velocity of 10 m s^{-1} for a) spherical, b) football, c) multibumps, d) golf ball, e) icosahedron, f) lattice, and g) square-patterned shot designs (Deformation scale factor = 1). All shots have a diameter of around 8 mm.

in MATLAB that followed the guidelines of the ISO standard for surface roughness description. The details of the code can be found in the author's previous study on classically shot peened surfaces.[27] The evolution of the roughness parameters as a function of impact number (directly related to peening coverage) at two different shot impact velocities is shown in **Figure 6**. The roughness evolution at high surface coverage levels with an impact velocity of 10 and 5 m s^{-1} (starting from the 30th and 24th impacts) is shown in Figure 6a,b, respectively. It is observed that regardless of the velocity, the spherical shot produced the lowest surface roughness at the studied coverage range. This can be justified by the geometrical features, which were added to the custom shots and contributed to further multiscale surface roughening.

The effect of a lower impact velocity (5 m s^{-1}) was investigated for only two of the custom shots (lattice and square patterned), as

depicted in Figure 6b. It was noticed that for these shots, the surface roughness was reduced almost by 50% for this lower velocity. However, in contrast to 10 m s^{-1}, the roughness trend with peening coverage showed less saturation, which may stem from a smaller indent depth and a higher required number of shots to cover the impact area. Although the simulations were not performed for the other custom shots at the velocity of 5 m s^{-1}, the same coverage trend can be hypothesized for them.

Figure 7 depicts the experimentally obtained surface textures produced by the slingshot system at three impact velocities of 5.6, 10.1, and 14.5 m s^{-1} and local coverage of ≈100%. Figure 7a shows the textures created by a spherical shot, while Figure 7b,c shows the textures by the as-built (AB) and polished icosahedron shots, respectively. LPBF materials are known to have poor surface quality, mainly caused by the presence of partially melted powders, and stepwise effects.[28] The polished shot
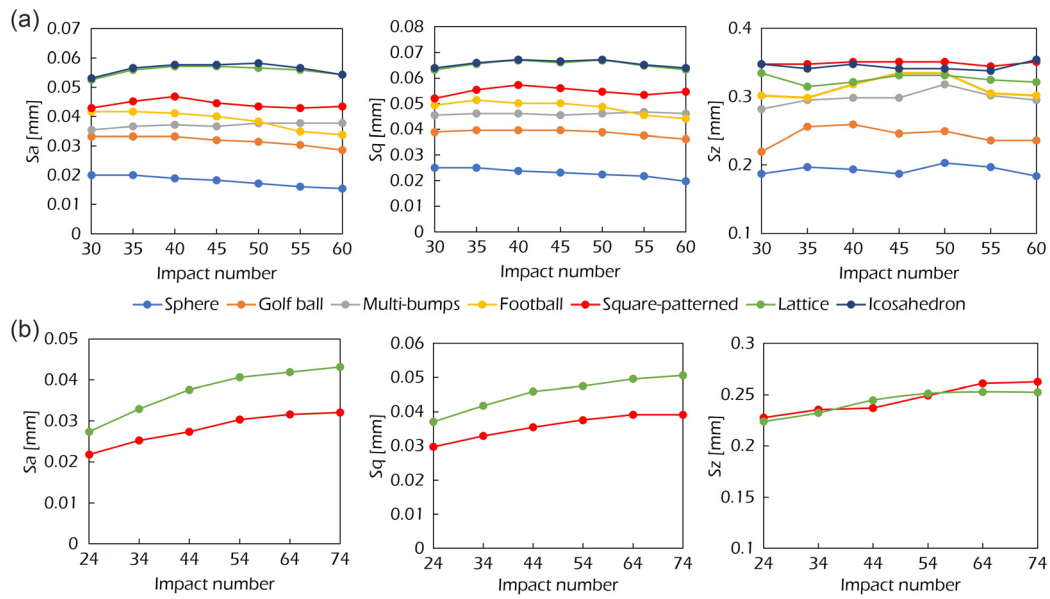
Figure 6. Evolution of the areal roughness parameters estimated by the FE model as a function of impact number with an impact velocity of a) 10 m s^{-1} and b) 5 m s^{-1}.
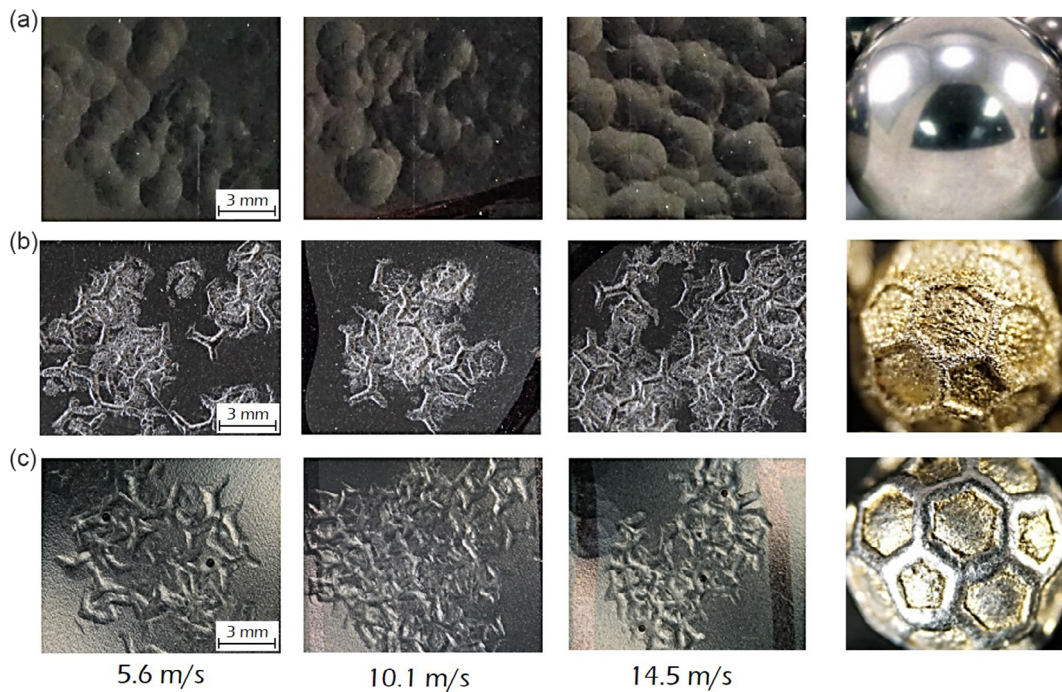
Figure 7. Top views of the experimental surface textures together with a close-up of the relevant shot with 60 shot impacts at impact velocities of 5.6, 10.1, and 14.5 m s^{-1} created by a) spherical shots, b) AB icosahedron shots, and c) polished icosahedron shots with a shot diameter of around 8 mm.

was intended to investigate the patterns by a customized shot with reduced surface roughness. The mechanical polishing of the AB shots was performed innovatively using a Retsch PM 400 Planetary Ball Mill. The custom-made shots were charged into the chamber and were rotated against each other at a rotary speed of 400 rpm for 30 min. The shots before and after polishing are inserted in Figure 7 for comparison.

To provide a quantitative comparison of the numerical and experimental textures, the areal roughness parameters extracted from the simulations were compared to those of the experimentally textured samples, focusing on the peened areas, as presented in **Figure 8**. The results obtained for the surfaces treated by spherical and the icosahedron shots are provided in Figure 8a,b, respectively. In the case of the spherical shot, the
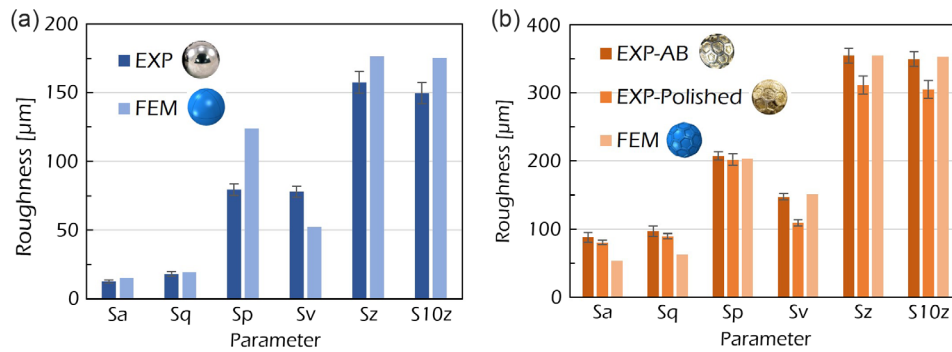
Figure 8. Comparison between the numerical finite element method (FEM) results of areal surface roughness parameters with an impact velocity of 10 m s^{-1} and experimental data (Exp) with an impact velocity of 10.1 m s^{-1} for a) spherical shot and b) icosahedron shot in the AB and surface polished states. The results correspond to 60 shot impacts.

data discrepancy on average is 8–18% for the global parameters (Sa and Sq) while some local parameters (Sp and Sv) show larger differences (around 33–56%) and some other (Sz and S10z) depict less (12–17%). For the AB icosahedron shot, the local parameters show a very good match (discrepancy less than 3%) while the numerical global parameters are 35–38% lower. As regards the polished icosahedron shot, the discrepancy for global parameters gets lower (30-33%) but the Sv parameter loses its good match (showing a 38% discrepancy) so a difference of about 15% is observed for Sz and S10z. In general, considering the random nature of the peening process and the wide range of impact angles that can occur in practice for the customized shots, the numerical results are matching well the experimentally measured surface roughness for both the spherical and icosahedron shots.

4. Discussion

In this study, a new texturing technique for polymeric materials is proposed using the conventional SP process combined with custom-designed shots.

The conventional surface roughness parameters were distinguished between the textured surfaces with those obtained by the basic spherical shot. In the case of peening with custom shots, the roughness parameters of Sa and Sq were found to be 2–3 times larger in comparison to the ones obtained by the spherical reference shot. However, the increase in Sz was less evident. This could be sensible since the added geometrical features to the custom shots contributed less to increasing the height of peaks or valleys, which determine the Sz parameter, but significantly increased the density of smaller features on the treated surface.

It is noted that at a high impact velocity of 10 m s^{-1}, the roughness parameters were already saturated with an increase in impact number in the studied range and were less influenced by peening duration (Figure 6a). There was even a slight decrease in Sa and Sq parameters with the increasing number of impacts. Saturation in the surface roughness parameters below full coverage has been investigated in the case of metals. It was shown for Armco iron that regardless of an inherent variation in the roughness parameters (such as Sa, Sq), due to random peening in terms of impact positions using spherical shots, the saturation
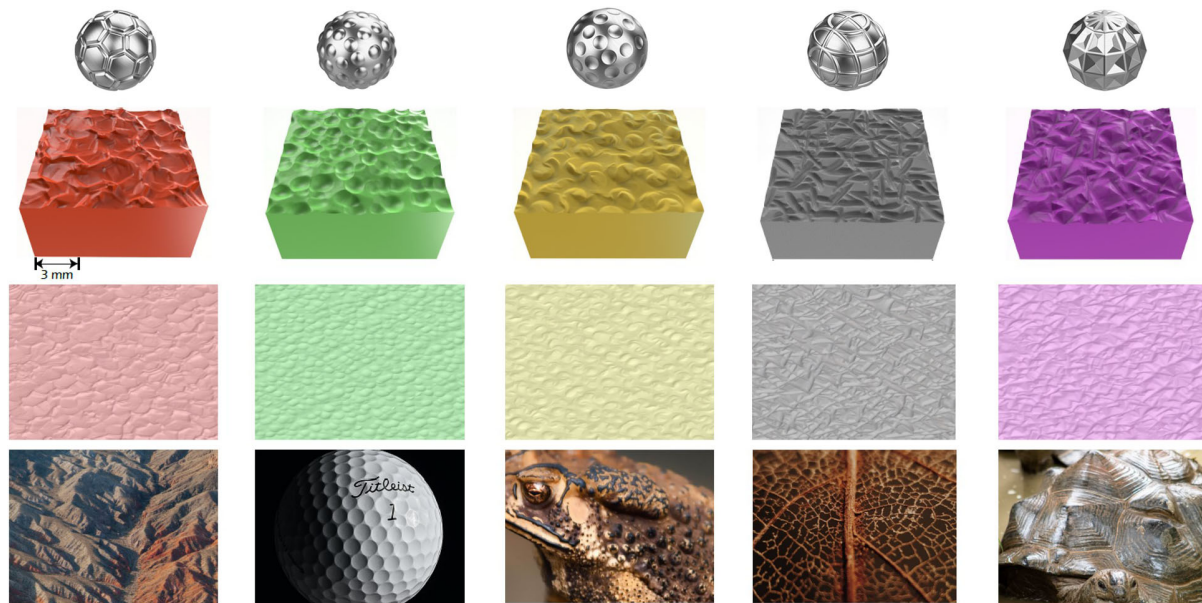
occurred at coverage levels higher than 50%, with even a decrease in the parameters within the coverage range of 50–100%.[27] Comparable behavior was detected in this study for the evolution of roughness parameters upon peening ABS polymer using custom-made shots.

The experimentally produced textures (Figure 7) were qualitatively comparable to their numerical counterparts (Figure 4). In general, it is observed that the experimentally formed features became larger/deeper for higher impact velocities. As also anticipated by the numerical simulation, the custom icosahedron shot was able to induce a distinctive texture in comparison to the classic SP morphology obtained using the spherical shot. The surface treated with the AB icosahedron shot (Figure 7b) appeared to show an additional small-scale roughness next to the larger indentations causing an opaque effect on the surface. This additional roughness was induced due to the rough nature of the shot in the AB configuration. By mechanical polishing, the surfaces of the shot became much smoother, leading to a textured surface without traces of tiny additional roughness. This aspect reveals a potential challenge in the surface texturing of polymers and requires further investigation regarding the postprocessing of the customized shots.

Fairly good agreement between the experimental and numerical surface roughness (Figure 8) indicates that the proposed SP numerical model works well in quantitatively predicting the produced textures. One of the main sources of inconsistency between numerical and experimental data could be the difference in the coverage parameter since it is quite difficult to control it in the preliminary experiments using the slingshot system. Another source of error could be the accuracy of the material model at very high strain rates (up to 10^6–10^8 s^{-1}) normally encountered in SP. The majority of the numerical roughness parameters for both the spherical and polished icosahedron shots were higher than the experimental parameters. Higher surface roughness is a consequence of material with lower mechanical behavior (caused by the utilized Johnson–Cook material model calibrated for low strain rates). One should not forget the uncertainty in the shot velocity estimation in the slingshot system as another probable source of error.

The sphere as the base shot model showed an acceptable match for the global roughness parameters despite the local

**ADVANCED
SCIENCE NEWS**

www.advancedsciencenews.com

**ADVANCED
ENGINEERING
MATERIALS**

www.aem-journal.com

Figure 9. Top row: FEM textures, middle row: photorealistic textures obtained by converting FEM results into seamless surface textures, bottom row: the inspired organic counterparts. All shots have a diameter of around 8 mm and the FEM textures correspond to 60 shot impacts.

parameters, which are normally more sensitive to the local variations of the surface pattern (Figure 8a). This match for global parameters deteriorated in the case of the icosahedron shot although shot polishing helped to reduce the discrepancy by enhancing the surface quality of the AB shot, making it closer to the ideally flat one in the numerical simulations (Figure 8b). Also, it is observed that the shot polishing had a certain effect on some of the local roughness parameters. This can be attributed to partial modifications in the dimensions of the features over the shot by mechanical work during ball milling.

Figure 9 shows the photorealistic rendered models of the simulated textures obtained after full coverage (60 impacts) at an impact velocity of 10 m s^{-1}. The deformed impact area was patterned to obtain continuous seamless surface textures capable of showing the expected aesthetic value of this texturing technique for each of the customized shots. The continuous surfaces show that depending on the geometry of the shot, different hierarchical structures can be obtained. The generated surfaces differ significantly from the surface produced by the reference sphere. It is pertinent to highlight the topographies obtained because they can be linked to organic surfaces in the real world and nature, as indicated in Figure 9, showing the ability to obtain nature-inspired surfaces. The textures produced by football, multi-bumps, golf ball, lattice, and square-patterned shots are assimilated just for the purpose of showing the vast range of inspirations, respectively, to a hilly landscape, the surface of a golf ball, skin of a toad, blade veins of a tree leaf, and hard shell of a musk turtle.

As introduced briefly in Section 2.1, the dimensions of the texturing media are dictated mainly by their fabrication technique, which requires a high resolution to create tiny features of the media. For this purpose, it will not be straightforward to take benefit of the more conventional air-blast SP process that

would require a large batch of customized media as well as very high air pressures to accelerate large and heavy custom shots. USP, on the other hand, has been used successfully for larger shots to mostly treat the flat and cylindrical parts.[18,29] In contrast to the SP, USP requires a very limited number of shots to be charged in an enclosed chamber. Given that the texturing was done on polymeric substrates at velocities as low as 1–10 m s^{-1}, minimum damage could be envisaged to the metallic shots with much higher hardness and strength than the substrate. Thus, the life cycle of custom media will be higher in comparison to conventional peening media.

The numerical simulations in this study show a high potential of the surface peening techniques to generate custom textures on the polymeric surfaces, depending on the final application and target functions. The proposed numerical approach provides an efficient tool for the exploration of the surface textures that could be generated using any potential design for the customized shot media.

5. Conclusion

The potential of the SP process to be used as a mechanical surface texturing method was investigated on polymeric substrates. A series of shot geometries were designed considering various target textures and taking into account the limitations of LPBF technology regarding the buildability of the features. Detailed FE models were developed to simulate multiple impacts of individual customized shot designs on the ABS polymer. On the basis of the present study, the following conclusions can be drawn. 1) The developed models demonstrated distinct surface textures that could be obtained as well as their evolution on the surface as a function of the number of impacts using

custom-made shots: this evidences a high potential of the surface peening techniques to generate custom textures on the polymeric surfaces, depending on the final application and target functions. 2) The numerical results compared with experimental data extracted from a series of preliminary tests performed with a customized additive-manufactured shot showed a satisfactory agreement, considering the uncertainties of the preliminary experimental tests. 3) The results revealed a high potential of SP to be paired with AM techniques to develop an efficient and cost-effective texturing methodology to control the surface morphology, not just for aesthetics but also to be expanded to more specific physical and mechanical functionalities, based on the final application.

Finally, it can be affirmed that the result of this study opens the view on the development of a new, flexible, economically, and environmentally sustainable process for surface patterning and functionalization.

Conflict of Interest

The authors declare no conflict of interest.

Data Availability Statement

The data that support the findings of this study are available from the corresponding author upon reasonable request.

[1] S. Bagheri, M. Guagliano, *Surf. Eng.* **2009**, *25*, 3.

[2] M. John, P. R. Kalvala, M. Misra, P. L. Menezes, *Materials* **2021**, *14*, 3841.

[3] C.-H. Su, T.-C. Chen, L.-W. Tsay, *Int. J. Fatigue* **2023**, *167*, 107354.

[4] C.-Y. Kang, T.-C. Chen, L.-W. Tsay, *Metals* **2023**, *13*, 69.

[5] M. Guagliano, *J. Mater. Process. Technol.* **2001**, *110*, 277.

[6] H. S. Abdul-Kareem, F. A. Abdulla, M. A. Abdulrazzaq, *IOP Conf. Ser.: Mater. Sci. Eng.* **2019**, *518*, 032017.

[7] H. Hadidi, B. Mailand, T. Sundermann, E. Johnson, G. Madireddy, M. Negahban, L. Delbreilh, M. Sealy, *Procedia Manuf.* **2019**, *34*, 594.

[8] C. Kanger, H. Hadidi, S. Akula, C. Sandman, J. Quint, M. Alsunni, R. Underwood, C. Slafter, J. Sonderup, M. Spilinek, J. Casias, P. Rao, M. P. Sealy, presented at *28th Annual Inter. Solid Freeform Fabrication Symp. - An Additive Manufacturing Conf., SFF 2017*, Austin, USA **2020**.

[9] J. S. Lee, R. T. Hill, A. Chilkoti, W. L. Murphy, in *Biomaterials Science*, 4th ed. (Eds: W. R. Wagner, S. E. Sakiyama-Elbert, G. Zhang, M. J. Yaszemski), Academic Press, Elsevier **2020**.

[10] A. F. Obilor, M. Pacella, A. Wilson, V. V. Silberschmidt, *Int. J. Adv. Manuf. Technol.* **2022**, *120*, 103.

[11] C. J. Barr, L. Wang, J. K. Coffey, F. Daver, *J. Mater. Sci.* **2017**, *52*, 1221.

[12] M.-X. Shen, Z.-X. Zhang, J.-T. Yang, G.-Y. Xiong, *Polymers* **2019**, *11*, 981.

[13] E. Maleki, N. Maleki, A. Fattahi, O. Unal, M. Guagliano, S. Bagherifard, *Surf. Coat. Technol.* **2021**, *405*, 126729.

[14] E. Maleki, M. J. Mirzaali, M. Guagliano, S. Bagherifard, *Surf. Coat. Technol.* **2021**, *408*, 126782.

[15] C.-S. Kim, S.-H. Ahn, D.-Y. Jang, *Vacuum* **2012**, *86*, 1014.

[16] A. Riveiro, A. L. B. Maçon, J. del Val, R. Comesaña, J. Pou, *Front. Phys.* **2018**, *6*, 16.

[17] S. S. Deshmukh, A. Goswami, *Mater. Today: Proc.* **2020**, *26*, 405.

[18] T. O. Olugbade, J. Lu, *Nano Mater. Sci.* **2020**, *2*, 3.

[19] G. Johnson, W. H. Cook, in *The 7th Int. Symp. Ballistics*, Hague, Netherlands **1983**.

[20] H. Louche, F. Piette-Coudol, R. Arrieux, J. Issartel, *Int. J. Impact Eng.* **2009**, *36*, 847.

[21] E. Nordin, B. Alfredsson, *J. Mater. Process. Technol.* **2016**, *235*, 143.

[22] F. Yin, Q. Han, M. Rakita, M. Wang, L. Hua, C., Wang, *Int. J. Comput. Mater. Sci. Surf. Eng.* **2015**, *6*, 97.

[23] S. C. Cao, X. Zhang, J. Lu, Y. Wang, S.-Q. Shi, R. O. Ritchie, *npj Comput. Mater.* **2019**, *5*, 36.

[24] D. Kirk, M. Abyaneh, *Shot Peener(USA)* **1995**, *9*, 28.

[25] A. Heydari Astaraee, R. Miresmaeili, S. Bagherifard, M. Guagliano, M. Aliofkhazraei, *Mater. Des.* **2017**, *116*, 365.

[26] ISO 25178-2 **2021**.

[27] A. Heydari Astaraee, S. Bagherifard, S. Monti, M. Guagliano, *Materials* **2021**, *14*, 3476.

[28] E. Maleki, S. Bagherifard, M. Bandini, M. Guagliano, *Addit. Manuf.* **2021**, *37*, 101619.

[29] J. Badreddine, S. Remy, M. Micoulaut, E. Rouhaud, V. Desfontaine, P. Renaud, *Adv. Eng. Software* **2014**, *76*, 31.